THE DAVID W. TAYLOR MODEL BASIN

UNITED STATES NAVY

PROPERTIES OF MEDIUM STEEL AT HIGH RATES OF LOADING

BY COMMANDER W. P. ROOP, USN AND ENSIGN HELEN I. CARRIGAN, USNR

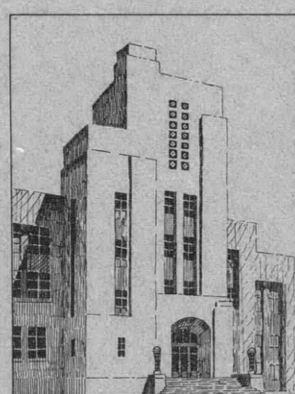

JUNE 1943

REPORT 503

RESTRICTED

NAVY DEPARTMENT

DAVID TAYLOR MODEL BASIN

WASHINGTON, D.C.

RESTRICTED

REPORT 503

PROPERTIES OF MEDIUM STEEL AT HIGH RATES OF LOADING

BY COMMANDER W. P. ROOP, USN AND ENSIGN HELEN I. CARRIGAN, USNR

JUNE 1943

PERSONNEL

The report was written by Commander W.P. Roop, USN, assisted by Ensign Helen I. Carrigan, USNR, with comments by A. Nadai. The digest is the work of Lieutenant Commander J. Ormondroyd, USNR.

DIGEST*

The David Taylor Model Basin first became concerned with tensile impact testing in connection with tests of structural models involving plastic action, specifically in the roller paths of gun and turret foundations. Conrad, on page 71 of a report dealing with this subject (13),** raised questions as to the dynamic similitude of the materials in the models. In particular he suggested that static tests would not be a safe guide in the prediction of plastic action under transient load, and especially that small-scale model tests might give erroneous indications of plastic action on full-scale structure in cases where the time rate of loading strongly affects the behavior of the metal.

In an effort to explore this field, a contract was made in 1939 by the Taylor Model Basin with the Massachusetts Institute of Technology for the prosecution of research on the properties of medium steel at high rates of loading. This work was continued during the fiscal years 1940, 1941, and 1942. Two reports were received, one as of 30 June 1941 (14), and one as of 30 June 1942 (15); these are available for consultation at the Bureau of Ships or at the Taylor Model Basin. The results obtained in the course of this work are presented here; they are compared with the results of other similar tests, and all results are reviewed and discussed.

However, these reports did not close the subject. On the contrary, the scope of the undertaking had by 1942 so widened that it was felt at the Taylor Model Basin that other agencies should be given a part in the project. After preliminary discussion with officials of the Watertown Arsenal, also interested in results of this kind, the Coordinator of Research and Development of the Navy Department was requested to consider plans for continuation of the work. This resulted in the formation of a project designated NS-109, under the auspices of the National Defense Research Committee, which took over supervision of the task as of 1 July 1942.

The present report is a critical review of the two MIT reports mentioned (14) (15). It gives an outline of the methods, procedures, and equipment used at the Massachusetts Institute of Technology for this project and a resume of the results obtained. This report also describes briefly similar work done by other investigators and gives a more extensive discussion and analysis of the MIT results than appear in the original reports.

---

* This digest is a condensation of the text of the report, containing a description of all essential features and giving the principal results. It is prepared and included for the benefit of those who cannot spare the time to read the whole report.

** Numbers in parentheses indicate references on page 32 of this report.

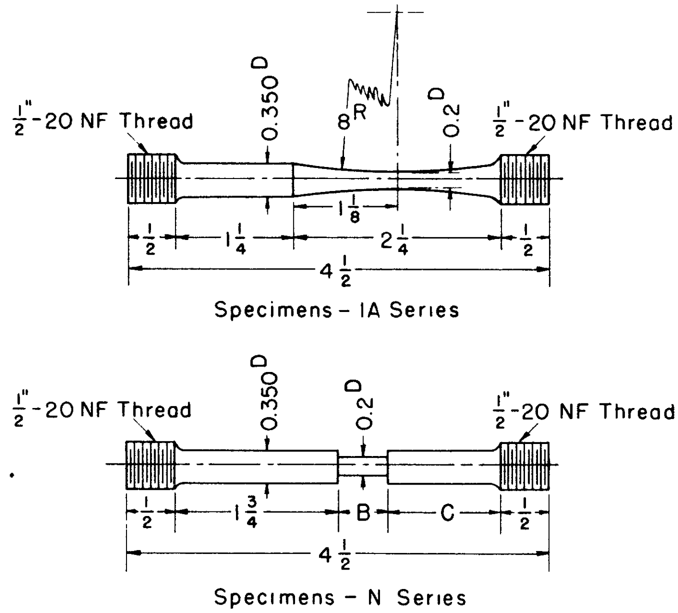

Series	B inches	C inches
1N	1/4	1 1/2
2N	3/8	1 3/8
3N	1/2	1 1/4
4N	3/4	1
5N	1	3/4
6N	1 1/2	1/4

Figure 1 - Detail of Specimens used in 1941 MIT Tests

All dimensions are in inches. The metalectric gages were applied to the cylindrical portions or "weigh bars" at the left which are 0.350 inches in diameter.

The MIT tests were carried out on uniaxial tensile test specimens. Figure 1 with its accompanying table, reproduced herewith, shows the shape and dimensions of the test specimens used up to June 1941. The 1-A scries of test specimens consisted of 12 exactly similar tapered specimens. The 1-N to 6-N series each consisted of 12 notched specimens.

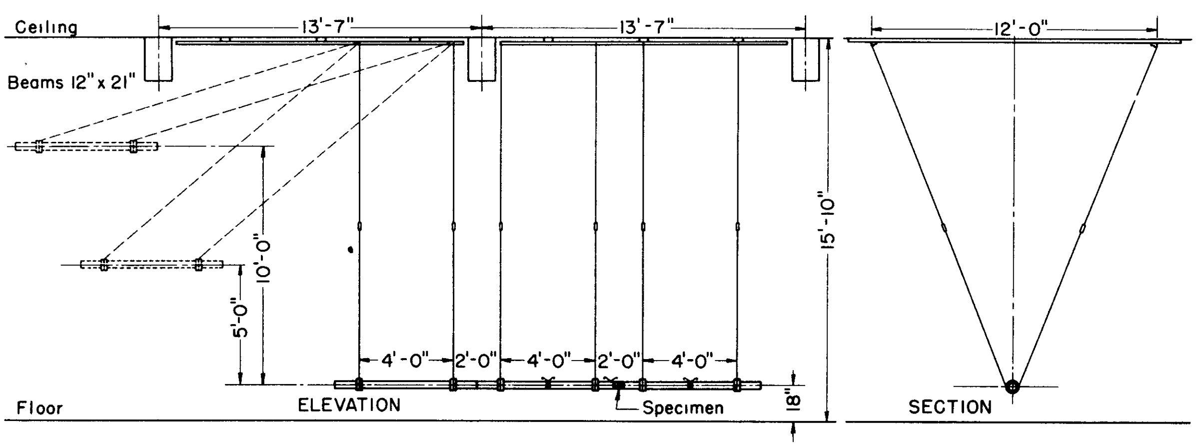

Three-Bar Impact Machine

The 3-bar machine comprises 3 equal 4-foot lengths of 2-inch round bar, each mounted on bifilar suspensions, all accurately aligned on the same axis. One is the hammer, the other two are joined by the specimen, until it is ruptured by the passage of a tensile wave through the bars. For details of the 3-bar machine, reference should be made to Figures 62, 63, and 144 of the original report. By this device strain rates approaching 1000 inches per inch per second were obtained.

This diagram was not included in the body of the present report but further consideration of the matter after the proofs were completed indicated that it might be shown here to advantage.

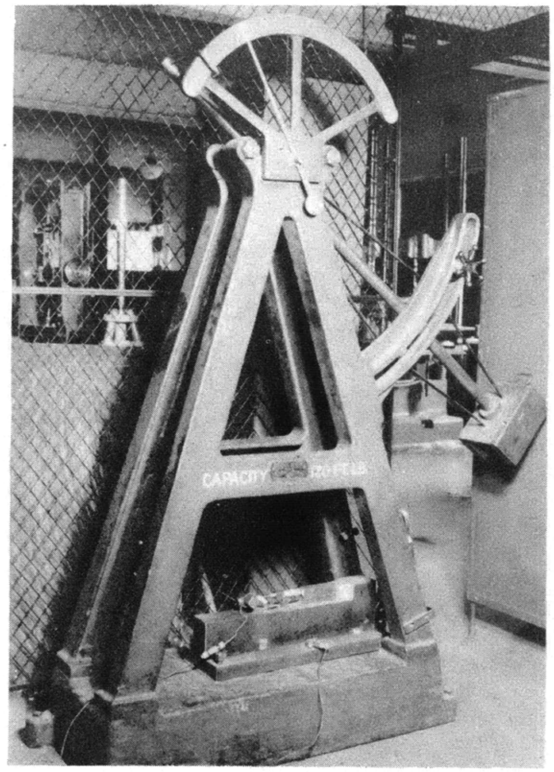

Converted Izod Impact Machine

The conversion appears to consist in substitution of the tensile assembly in place of the usual Izod clamp. This photograph was not included in the body of the present report but further consideration of the matter after the proofs were completed indicated that it might be shown here to advantage.

Some of these specimens were subjected to static tests in an ordinary tensile test machine; some were loaded rapidly in a converted Izod impact machine, and some were loaded rapidly in the MIT three-bar impact machine. All were loaded up to failure.

In the tests reported in 1942, 16 tapered tensile specimens were tested and 6 series of notched tensile specimens with different notch lengths. Each series of notched specimens consisted of at least 2 specimens; one was tested statically, the other at a high rate of loading. All the specimens tested dynamically in this group were pulled apart in a bomb-type impact tester, described on page 14 of this report and shown in Figure 8, page 14.

The three-bar impact machine and the bomb-type impact tester were innovations of loading equipment introduced by the Massachusetts Institute of Technology. The means of measuring load, total elongation and strain were also novel for the high strain rates used. The load was measured by a resistance-sensitive strain-measuring wire pickup,* firmly cemented to a "weigh-bar" section included in one end of each specimen tested; see Figure 1 and the comments on pages 3 and 4 of this report.

From simultaneous records of load and elongation, the orthodox type of stress-strain curve shown in Figure 2 can be deduced. By a suitable procedure as described on pages 6 and 7, employing the actual area of the specimen A instead of the original area A_0, "true" stress-strain curves can also be produced. A special measuring technique, including the use of tapered specimens, shown in Figure 1, indicated the distribution of strain in the plastic range of deformation.

The notched specimens were used chiefly to measure energy absorption in the rupturing process.

---

* These are widely known now under the commercial name of SR-4 metalectric wire strain gages.

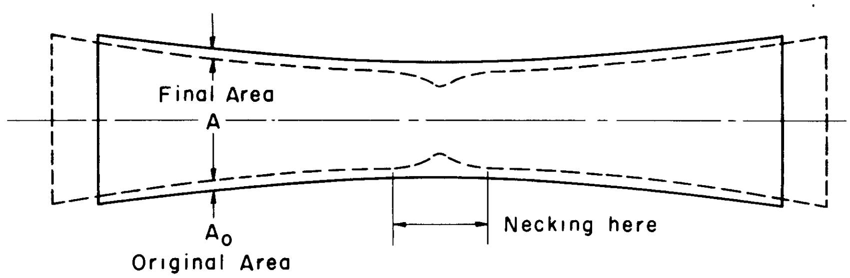

Figure 4 - Diagram illustrating Deformation in a Tapered Specimen under Impact Load

Circumferential lines were scribed around the specimen, spaced closely (0.1 inch apart) at the central small diameter section of the tapered specimen. From measurements of diameter at these stations, true strain could be deduced even in the necked section of the specimen.

A thorough understanding of the concepts of "true" stress and "true" strain as described on pages 5 to 11 and in the Appendix of this report, are important to a complete understanding of this project, and the reader is advised to read them in full at this point.

The original test data of the MIT reports are not reproduced in their entirety in the present TMB report; typical examples of the test data and the results are given instead. The original photographic data on the load-time relationship for notched specimen 1 N-6 are given on page 11. Table 1 is a complete "Index to Tensile Impact Data in the 1941 MIT Report." Figures 9, 10, and 11 on pages 15, 16, and 17 are examples in curve form of the type of data observed at the Massachusetts Institute of Technology. Table 3 on page 18 gives an "Index to Tensile Impact Data in the 1942 MIT Report," and Figure 12 on page 19 summarizes in curve form the data in the relationship between the ratio of true dynamic fracture stress to static value and the strain rate at fracture for specimens tested in 1942.

In an attempt to assess the significance of the mass of available data, the present report puts great emphasis on the concept of energy absorbed, in inch-kips per pound of metal, in the fractured test specimen. Table 2 on page 16 shows for some of the tapered specimens ruptured in the bomb impact machine the relationship between energy absorbed and fracture load at various rates of loading. This table shows in general that the energy absorbed to fracture rises with the rate of loading. Table 4 on page 19 shows the energy absorption per pound of metal at the breaking section under static loading for 14 specimens and indicates on the average that fracture occurs when about 440 inch-kips per pound have been absorbed at the breaking point.

The energy absorption per pound, taken over the whole gage length of the notched specimens, is lower than this limiting value even under dynamic loading since the material of the unnecked section is included. This is shown in Figure 13 on page 21, which also indicates that the specific energy absorption rises with increasing strain rate. Figure 14 shows that energy absorption increases with the notch length in the notched specimens and Table 5 on page 20 gives detailed data on the relationship between notch length, strain rate and specific energy absorption. Table 6, reproduced here, shows the specific energy for tapered specimens tested up to 1941.

TABLE 6

Energy Absorption Ω at Section of Greatest Strain in Tapered Specimens

1941 MIT Report

inch-kips per pound of metal

Specimen	Ω	Specimen	Ω
1-A3	539	1-A9	441
1-A4	618	1-A10	426
1-A6	684	1-A11	477
1-A7	494	1-A12	630
1-A8	430		

Table 7 on page 23 shows energy absorption data from experiments made by Nadai in a flywheel impact machine at the Westinghouse laboratories. Figure 15 on page 26 summarizes energy data, notch length and rate of loading in tests made by Duwez at the California Institute of Technology.

The general conclusion which can be drawn from these tests is that mild steel shows an increase of energy absorption with increasing strain rate, but the difference between static and high speed loading will hardly exceed 50 per cent. The limiting values obtainable locally, at the rupture point, may be 500 inch-kips per pound of metal. Averages taken over a whole specimen may be in the order of only 1/50 as much; in an extended assembled structure the averages may be expected to fall still lower. From this point of view there is thus almost limitless room for an improvement in the efficiency of structures such as torpedo protection systems.

If a modification of practice could increase the energy absorbing capacity of a ship's side by 1/20 the figure attained in the neck of a tensile specimen, the result would be a revolution in sea warfare.

PROPERTIES OF MEDIUM STEEL AT HIGH RATES OF LOADING

ABSTRACT

The history of impact testing is briefly stated, with references, and two reports by the Massachusetts Institute of Technology are reviewed in some detail. The idea of true stress and true strain and MacGregor's work in this field are discussed at length. Other sources of information are also drawn upon. Interest is centered on the plastic absorption of energy and it is noted that great benefit would accrue from any practice that would increase the capacity of a ship structure for plastic deformation before rupture.

INTRODUCTION

Two aspects of the impact testing of steel must be distinguished. The first refers to a quality of the material, its brittleness;* the second aims at evaluating its resistance to shock loads in service.

When a notched bar is broken in bending by a blow, as in the Charpy test or the Izod test, a skilled metallurgist knows by the appearance of the fracture whether the desired quality in the metal has been obtained. A numerical scale of energy absorption in standard specimens exists, but numbers on this scale have only relative meaning and "cannot be used directly in design" (1).** Tests of this nature have been used in practice for many years (2) and many attempts have been made to reduce quantitative data of the sort thus obtained to more significant form. Recently a renewed effort of this sort (3) marked a revival of interest in the subject. Useful summaries have appeared in the literature (4) (5) (6). Similitude has received special consideration by Nadai and MacGregor (7).

Although energy absorption in notched bar specimens broken by impact has been brought to the point of extensive systematic measurement, it still cannot be said that a rational measure of impact strength, expressible in suitable terms for dimensional operations, has emerged from this work. Such a result is more nearly attained in projects of the second sort, also foreshadowed by the work of H.C. Mann (3). Tensile specimens were used, and emphasis was placed on the effect of varying the velocity of impact.

It soon appeared,† however, that the measurement of energy absorption as accomplished by Mann (3) was not adequate for the purpose of defining

---

* From the beginning we must avoid the error of supposing that brittleness is a property inherent in the material; the amount of plastic flow before rupture, or ductility, depends also on the conditions of loading, the constraint, and the form of specimen. In comparisons such as those made in the standardized Charpy test, all these conditions must be exactly controlled.

** Numbers in parentheses indicate references on page 32 of this report.

† E. Lehr (8) states; "It is not possible that energy absorption should decrease with increasing speed of loading if the elongation remains unchanged or increases, as Mann has asserted."

the behavior of steel at high rates of loading, and the difficult task of obtaining stress-strain curves in tensile impact became necessary.

A paper by Clark and Dätwyler published in 1938 (4) marks a recurrence in the United States of interest in data of this kind. These experimenters made use of a dynamometer for recording the rapidly varying load on the specimen, in which an old principle is given a novel application. The principle is that by which the ohmic resistance of a metallic wire varies when its dimensions are altered, as by isotropic pressure on the wire, or by simple tension. The new use of this principle is effected by securing the wire to a solid surface by an insulating adhesive; strain in the solid is then shared by the wire with a minimum of disturbance such as is caused by hysteresis, inertia, and the like. At the same time work with the same purpose, but using different methods, was being carried on by Nadai and Manjoine (9) (10), who also used a force-measuring bar; its elastic elongation, however, was recorded by a photoelectric system.

In the meantime this problem was also taken up by Ruge and deForest at the Massachusetts Institute of Technology, where development of the resistance-sensitive strain pickup was actively pursued and given a turn in the direction of standardization and quantity production. The commercial rights of all hands, insofar as patentable claims exist, were gathered together by the Southwark Division of the Baldwin Locomotive Works, under the trade name "SR-4 Gage";* the gage operates on the "metalectric" principle. The David Taylor Model Basin has been licensed by Baldwin-Southwark to utilize the principles and processes covered by pending patents, if they are subsequently issued.

In addition to the direct experimental work of impact testing, the phenomena involved have received attention from the theoretical side; the problem has been stated in terms of the distribution of permanent strain remaining in a linear bar after passage of a plastic wave. The most recent papers in this vein are those of Bohnenblust (11) and Duwez (12), in which references to previous work by von Kármán, Griffis and White, Donnell, and others will be found.

The David Taylor Model Basin became first concerned with tensile impact testing in connection with model tests of structure involving plastic action, specifically in gun and turret foundations. Conrad, on page 71 of his report (13), raised questions as to the dynamic similitude of materials. In particular he suggested that static tests would not be a safe guide in the

* S stands for Simmons, R for Ruge, and 4 for other collaborators.

prediction of plastic action under transient load, and especially that small-scale model tests might give erroneous indications of plastic action on full-scale structure in cases where the time rate of loading strongly affects the behavior of the metal.

In an effort to explore this field further, a contract was made in 1939 by the Taylor Model Basin with the Massachusetts Institute of Technology for the prosecution of research on the properties of medium steel at high rates of loading. This work was continued during the fiscal years 1940, 1941, and 1942. Two reports were received, one as of 30 June 1941 (14), and one as of 30 June 1942 (15); these are available for consultation at the Bureau of Ships or at the Taylor Model Basin. Reviews of these reports will now be given, after which the results obtained will be presented, compared with the results of other similar tests, and all results will be discussed.

However, these reports did not close the subject. On the contrary, the scope of the undertaking had by 1942 so widened that it was felt at the Taylor Model Basin that other agencies should be given a part in the project. After preliminary discussion with the Watertown Arsenal, the Coordinator of Research and Development of the Navy Department was requested to consider plans for continuation of the work. This resulted in the formation of a project designated NS-109, under the auspices of the National Defense Research Committee, which took over supervision of the task as of 1 July 1942.

REVIEW OF 1941 AND 1942 REPORTS

Two major reports (14) (15) have been rendered by Professor A.V. deForest and assistants of the Massachusetts Institute of Technology, one in 1941 and one in 1942. These are concerned mainly with details, and present no incisive picture of the problem and its partial solution.

1941 MIT REPORT

Pickups

The 1941 MIT report opens with a detailed account of the construction and use of the "gages," i.e., the resistance-sensitive strain-measuring pickups.

The change with strain in the resistance of the pickup unit is small, and temperature changes are therefore important; these are compensated by the use of wire with low temperature coefficient, and by the use of bridge arrangements in which a partial cancellation occurs. In the case of rapid action the mechanical deformations are accompanied by adiabatic thermal effects not separately accounted for. In the report no systematic numerical data are given; in particular no evidence is offered as to the variation of pickup sensitivity with frequency. Other incidental effects, such as hysteresis, acceleration response, and in general the fidelity with which resistance change in the wire reflects strain in the base metal, are not mentioned.

From purely geometrical considerations of the performance of this pickup, if the volume of metal were constant the fractional change in resistance would be double the strain, since the resistance is increased both by the increase in length and the decrease in area. The ratio of the change in resistance to strain is observed to exceed 2; in the case of "isoelastic steel" it rises to 3.7; but in Advance wire, commonly used, its value is only 2.16. This is said to be constant far into the plastic range, at strains up to 4 per cent.

Recorders

The signals received from these pickups are faint and require amplification by electronic methods. These are discussed at length in the MIT reports, but a shorter description of similar practice at the Taylor Model Basin may be found in a TMB report (16).

Explosion Pressure

The proposed use of explosion pressure waves in water for obtaining the highest rates of loading on steel specimens led to some effort to adapt the metalectric principle to use in a gage for measuring pressure in such waves. Extensive work of similar nature at the Taylor Model Basin will be separately reported; the work reported by the Massachusetts Institute of Technology furnished suggestive indications as to experimental methods, but it did not pursue the matter to a conclusion. In connection with the main purpose of the project, purely mechanical methods of loading were used.

Tensile Impact Tests

The main substance of the 1941 MIT report is entered under this heading. Seven series, each consisting of twelve specimens, were tested; these are pictured in Figures 147 to 153, on pages 130 and 131 of the 1941 report. Series 1N to 6N are notched, Series A is tapered; details of the specimens are sketched in Figure 146 of the report, reproduced here as Figure 1. In the notched specimens the notch length varied from 1/4 inch to 1 1/2 inch. Hammer speeds in the Izod machine varied from 45 to 125 inches per second so that strain rates could be pushed up in the short notches to a nominal 500 inches per inch per second.

In each series of twelve, two specimens were given a static test, and the remaining ten were loaded by impact either in the Izod or in the

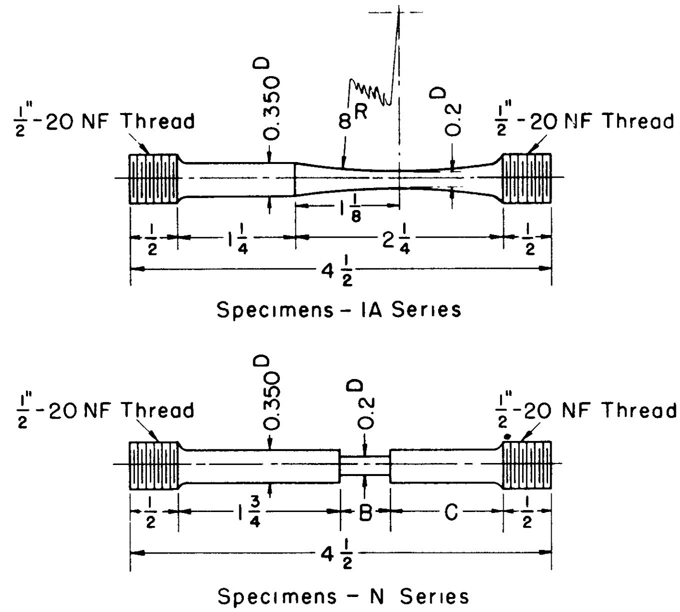

Series	B inches	C inches
1N	1/4	1 1/2
2N	3/8	1 3/8
3N	1/2	1 1/4
4N	3/4	1
5N	1	3/4
6N	1 1/2	1/4

Figure 1 - Detail of Specimens used in 1941 MIT Tests

All dimensions are in inches. The metalectric gages were applied to the cylindrical portions or "weigh bars" at the left which are 0.350 inches in diameter.

"3-bar" machine. The 3-bar machine comprises 3 equal 4-foot lengths of 2-inch round bar, each mounted on bifilar suspensions, all accurately aligned on the same axis. One is the hammer, the other two are joined by the specimen, until it is ruptured by the passage of a tensile wave through the bars. For details of the 3-bar machine, reference should be made to Figures 62, 63, and 144 of the original report. By this device strain rates approaching 1000 inches per inch per second were obtained.

The tapered specimens were made up and tested in accordance with MacGregor's "two-load method" (17) for obtaining a stress-strain curve by measurements of plastic reduction in area of the specimen after rupture. In the case of the two specimens tested statically, opportunity was taken to obtain a confirmation of the validity of the two-load method.

True Stress and Strain

For a full understanding of the analysis to follow, it is necessary to have a clear picture of the procedure and reasoning involved in this two-load method, and a definite understanding of the terms "true stress" and "true strain," as MacGregor uses them. This can perhaps best be set forth by considering briefly a few of the principles involved in the orthodox procedure of testing materials.

Consider the cylindrical portion of a standard test specimen, as shown by the full lines of Figure 2, where the original length is L_o and the original area is A_o. The specimen is subjected to a static test, during the course of which the material between the gage points stretches elastically with load from O to P, then yields at Y. Beyond this point the cylinder increases in length and decreases in diameter by uniform plastic flow. In spite of the loss in diameter, strain-hardening makes the material capable of taking a gradually increasing load, up to M. At this point the plastic deformation ceases to be uniform and necking begins, the load begins to fall off, and finally rupture occurs at F. When the load has again dropped to zero, a slight amount of elastic strain left in the specimen causes it to shorten to its final length at F_1. Actually the specimen was longer at F, but as this length cannot conveniently be measured, the length at F_1 is used in all ordinary calculations and the springback F_1F_2 is neglected. It is likewise neglected in the analysis in in this report.

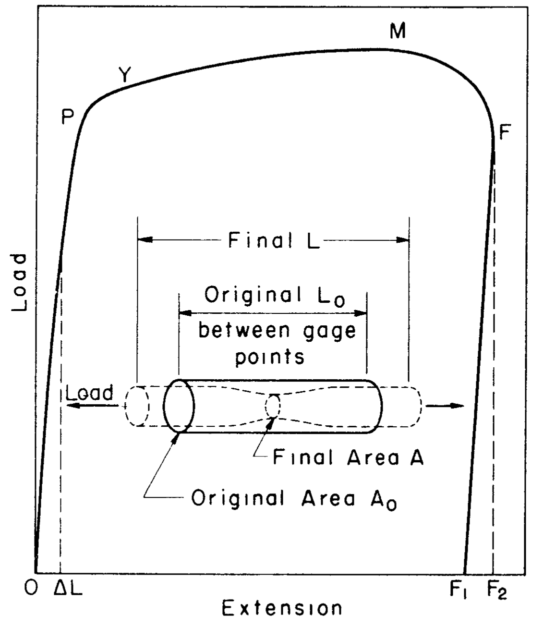

Figure 2 - Load-Extension Diagram of a Specimen Loaded to Fracture

Actually, the extension represented by OF_1 on the curve is equivalent to the extension $L - L_o$ of the specimen.

According to the customary method, the small elastic strains in the region below P are now found by evaluating the fraction $\frac{\Delta L}{L_o}$. Following that precedent, the much larger final elongation is expressed by the fraction $\frac{OF_1}{L_o}$ or $\frac{L - L_o}{L_o}$, and the final reduction in area by $\frac{A_o - A}{A_o}$. It will be noted particularly that in each case the divisor is the *original* length or area. The use of this figure is a great convenience in working up the data, but it will be appreciated that this procedure is somewhat arbitrary and artificial when applied to the large fractions involved in plastic action.

It will be noted that strain, considered as a change in length, has a certain relation to the transverse action considered as reduction in area. Below the proportional limit this is expressed in terms of Poisson's ratio, the value of which for steel is about 0.3. In the plastic region under consideration here, however, in the region beyond Y in Figure 2, it has been found by experiment (22) that Poisson's ratio is about 0.5 for steel. This,

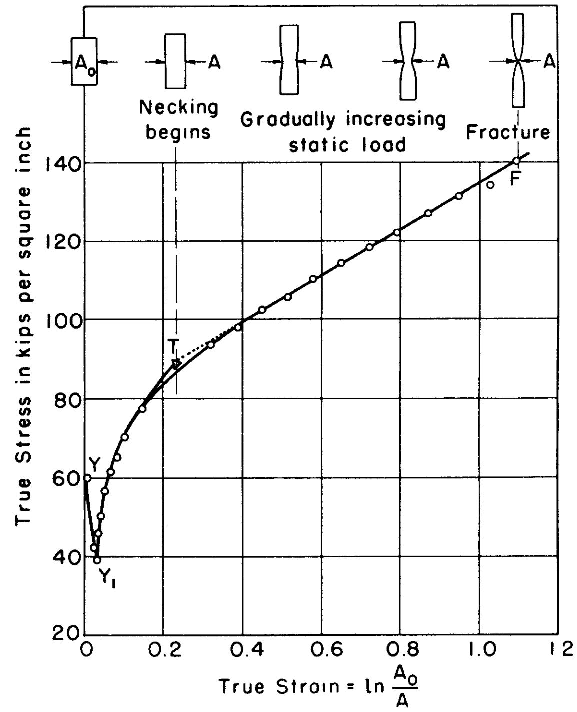

Figure 3 - Typical Curve of True Stress and True Strain observed under Static Loads

The load and area at the transition point **T** and those at the fracture point **F**, combined with the experimental determination that the line joining them in this diagram is straight, form the basis for the term "two-load method."

The open circles are plotted from true plastic strain data taken at the minimum section at each of a series of static loads, as shown here and as tabulated on page 150 of the 1941 MIT report. The transition point **T** is shown in Figures 3 and 6 at the break in the dotted line. In the 1941 report a faired curve was drawn at the transition and this is shown in Figures 3 and 6 as a solid line.

Actually, the short test section shown is the central part of a long specimen, as illustrated in Figure 1. In MacGregor's method a tapered specimen is used for reasons explained later in this report.

expressed in other terms, means that the volume of any element in the test section remains constant, or that, for the final condition shown in Figure 2, $AL = A_0 L_0$. Thus, by measuring the change in diameter of a specimen of circular section at any value of load in the plastic region, a procedure not too difficult in a static test,* the change in length, and hence the strain, can be determined. By the process described in the Appendix on page 35, it is then possible to express the true strain $\epsilon = \ln \frac{L}{L_0}$ as the same function of the reduction of area, $\epsilon = \ln \frac{A_0}{A}$, and by measuring diameters to determine ϵ. Knowing the true diameter A for every load, it is possible to calculate and plot the true stress; the data for a true-stress - true-strain curve are thus available.

Now turn to the procedure devised by MacGregor for plotting true stress on true strain by observation of two load values only. Part of Figure 156 of the 1941 MIT report is reproduced here in Figure 3. The course of the true-stress - true-strain curve was found by measurement of diameter at the minimum section at a series of static loads, and the results are plotted as open circles. The line TF is seen to be quite straight. On the other hand, MacGregor takes the necessary data for determining only the two points T and F, and fills in the curve by constructing a straight line joining them. By

---

*This necessitates a temporary cessation of movement of the straining heads relative to each other.

determining the load at the rupture point F, and dividing it by the area of the minimum section after rupture, he finds the end point of the true-stress - true-strain curve for that section. Connecting this with the transition point T in Figure 3 by a straight line, he completes the curve of true stress on true strain. The correctness of this procedure is confirmed by the fact that a straight line drawn from T to F agrees well with the positions of the open circles.

The points Y and Y_1 show upper and lower yield points not relevant to the form of the curve above the transition point.

The foregoing remarks apply to the analysis of static tests on a specimen, where the corresponding loads and areas in the specimen can be measured at a number of points on the load curve.

Consider now the specimens tested under impact, where it is possible to measure only the initial areas before the test and the final areas after rupture is complete, and no intermediate values. It is assumed that the straining heads of the testing machine move at a fairly uniform rate and that the rate of elongation of the whole specimen remains nearly constant. When necking begins, the load diminishes and the elongation is concentrated in a short length of the specimen, while in the rest of the specimen the plastic flow ceases. By employing a tapered specimen, MacGregor makes use of this fact to find the maximum stress reached at each of a series of sections under the maximum load; these maximum stresses at the several points in the specimen differ because of the differences in sectional area. The maximum load withstood, which is the same at all points along the specimen, caused the sections along the specimen to contract by varying amounts, depending upon the maximum stresses reached at the various points; the stresses produced by this load vary inversely as the area along the tapered specimen. Now the measurement of the maximum load and of the original and final areas at a series of points, as shown in Figure 4, permit the plotting of an approximate true-stress - true-strain curve for an impact-loaded specimen. This procedure is naturally possible also in a static test, but it is all that is possible in an impact test. A sample curve, also taken from Figure 156 of the 1941 MIT report, is reproduced here as Figure 5.

If the profile of the necked metal slopes gradually to the section of rupture, as shown in Figure 4, a number of spots, calculated as described, will fall above the transition point and flow at these points continues after load reaches the peak value. The ordinates of the spots in Figure 5 above the transition point are obtained by the nominal assumption that reduction of load beyond the maximum may be ignored; a rough value of true stress is

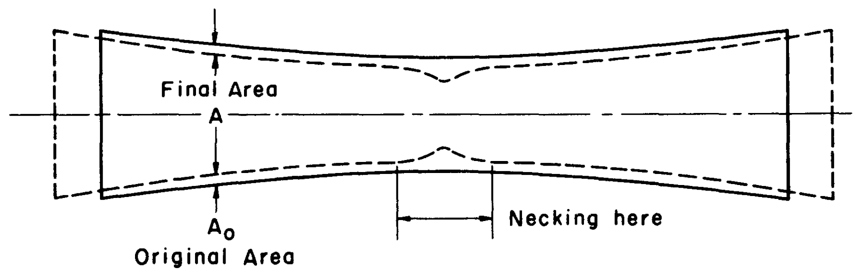

Figure 4 - Diagram illustrating Deformation in a Tapered Specimen under Impact Load

The diameters A_0 and A are measured along the tapered length at as many stations as may be desired, before and after the fracture, respectively.

then estimated for each spot by dividing the maximum load by the area at the corresponding section. In this way the broken line of Figure 5 was traced from the data on page 164 of the 1941 MIT report. However, it is clearly only approximate.

If now, the curves of Figures 3 and 5 are combined, as shown in Figure 6, it will be found that up to the transition point, or perhaps slightly above it, they coincide quite well. But above the transition point the approximate curve based on ignoring loss of load during necking is seen to be definitely too high. Now if in addition to the maximum load the fracture load can also be measured, MacGregor's straight line construction is possible, and its validity, at least in the static case, is demonstrated by the agreement of the full line with the open circles in Figures 3 and 6.

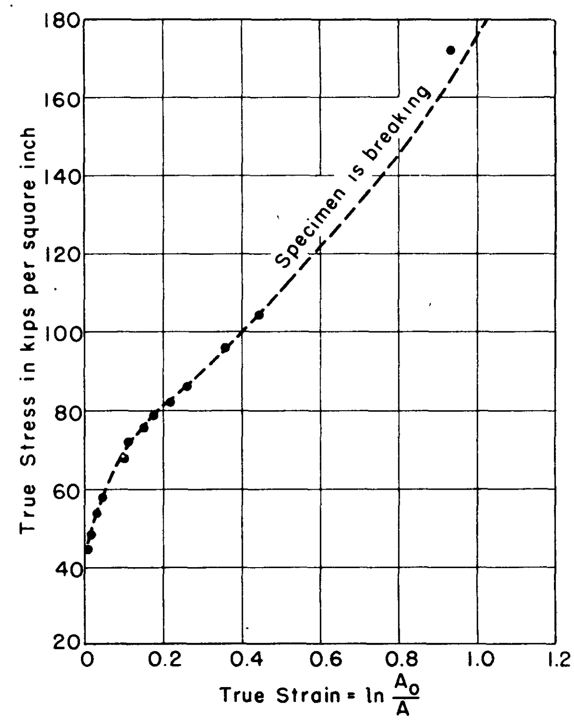

Figure 5 - Approximate Curve of True Stress and True Strain inferred from observation of Maximum Load

All measurements for this curve were made after rupture. Each spot refers to a different section of the tapered specimen.

The principal feature of these curves is the continued rise of stress with increasing strain; this is the simple result of allowing for reduction of area in computing stress, instead of dealing in terms of gross

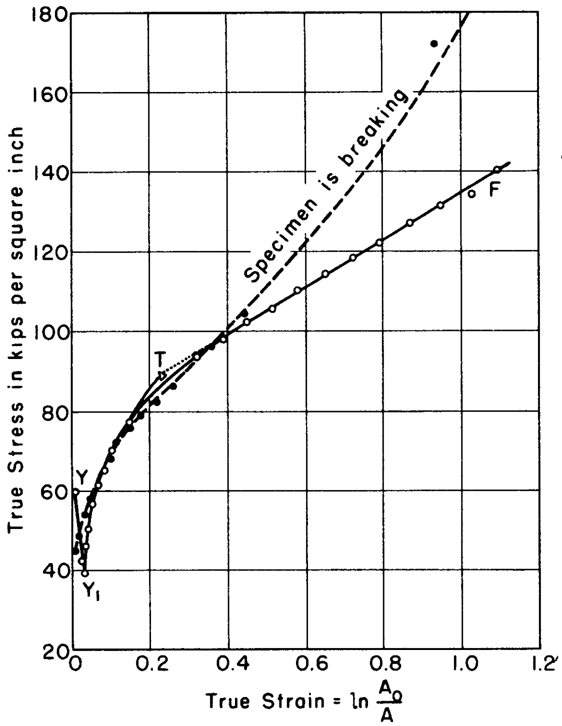

Figure 6 - Typical Curve of True Stress and True Strain illustrating MacGregor's Method

The full-line curve shows true stress at the minimum section as obtained by MacGregor's method. The points represented by the open circles were obtained from measurements of diameter at a series of static loads. The broken-line curve faired through the solid circles shows the quotient of maximum load divided by sectional area in the tapered specimen corresponding to the plotted strain value. The two curves approximately coincide at stress and strain values below maximum load represented by the point of inflection in the upper curve. See also notes to Figure 3.

load and original area and so ignoring the whole phenomenon of necking.

The curve obtained from the plastic strain under static load at the minimum section, as shown by the open circles of Figure 6, shows an upper and a lower yield point, Y and Y_1, whereas that shown by the solid circles does not. The yield point in medium steel has had great significance, even if only as a stress well defined numerically which serves as an extreme limit of acceptable working stress. In point of fact, however, the yield point, as defined in the standard static tensile test, is very often exceeded in service. Either or both of two things may happen: the resulting plastic flow may equalize stresses about a small area of concentration, or it may cause a rise in yield stress through strain hardening. The continued rise of stress with increasing strain in Figure 6 gives a clear picture of the process of strain hardening, and in this way receives an explanation which for ordinary purposes is completely adequate.

For structures in which rigidity is an essential feature, and in which permanent or residual deformation after strain interferes with subsequent functioning of the structure, the use of yield point as a limit for working stress is quite rational. The benefits of strain hardening are then to be obtained only by some pre-stressing process.

But in structures like underwater explosion protection systems, in which plastic action is certain to occur in an emergency, the use of the yield point taken from a standard static tensile test represents only a rough preliminary approximation and a nominal treatment of the matter. To ignore the effects of strain hardening is to omit one of the most potent aids enjoyed by medium steel subjected to plastic action.

The type of stress-strain curve illustrated in Figure 6 is thus especially significant for cases in which plastic action predominates.

Notch Length

Some of the notched tensile specimens appear to have been tested in the Izod machine and the energy absorption measured in the usual way; the results are plotted in Figure 155, page 133 of the 1941 MIT report. These data cannot be identified with any mentioned elsewhere in that report. The energy absorption in foot-pounds is said to be $70\, l^{0.7}$, where l is length in inches. It is noted, however, that the quantity energy absorption per pound of metal in a notch of very small length would be expected to approach a finite value. Now this quantity is proportional to the slope of the curve of total energy absorption on length, and in the given simple power function this slope becomes infinite at zero value of l. A more correct alternative expression fitting the same data is given in Figure 9 on page 15 of this report.

The 1941 MIT report also contains other groups of data on energy absorption as indexed here in Table 1, page 12.

Nature and Treatment of the Tensile Impact Data

The character of the data obtained is indicated in Table 1. In all tensile impact tests an oscillographic record of load on time was obtained, and these oscillograms, to the number of 71, are reproduced in the 1941 MIT report. This represents a large amount of effort and the records set a high standard of oscillographic work. The record for Specimen 1N6, Figure 80 of the report, is reproduced herewith in Figure 7; it is typical, and not better

Figure 7 - Sample Oscillograph Record of Specimen 1N6 showing Load plotted on a basis of Time during Elongation

This is Figure 80 of the 1941 MIT report.

Yield Point Load (highest peak)	4550 pounds
Maximum Plastic Load	3500 pounds
Fracture Load	2280 pounds
Average Load (taken on time base)	2980 pounds

TABLE 1

Index to Tensile Impact Data in the 1941 MIT Report

Designation	Photo of Specimens		Length of Notch inch	Static Data Recorded on page	Static Data Plotted		Impact Data Recorded on page	Oscillograms		Energy Data on page	Energy Data Obtainable	
	Figure*	Page			Figure	Page		Figure	Page		Figure	Page
1-A 1 to 12	147	130	Tapered	164-165 150-151	156 to 157	134 to 135	166-175 188	67 to 75	106 to 108		156 to 157	150 to 151 164 to 175
1-N 1 to 12	148	130	1/4	152-153	158 to 159	136 to 137	176, 182, 189, 191	77 to 88	109 to 111	191 133 182	158 to 159	152 to 153
2-N 1 to 12	149	130	3/8	154-155	160 to 161	138 to 139	177, 183, 189, 191	89 to 99	112 to 114	191 133 183	160 to 161	154 to 155
3-N 1 to 12	150	130	1/2	156-157	162 to 163	140 to 141	178, 184, 189, 191	100 to 110	115 to 117	191 133 184	162 to 163	156 to 157
4-N 1 to 12	151	131	3/4	158-159	164 to 165	142 to 143	179, 185, 190, 192	111 to 122	118 to 120	192 133 185	164 to 165	158 to 159
5-N 1 to 12	152	131	1	160-161	166 to 167	144 to 145	180, 186, 190, 192	123 to 133	121 to 123	192 133 186	166 to 167	160 to 161
6-N 1 to 12	153	131	1 1/2	162-163	168 to 169	146 to 147	181, 187, 190, 192	134 to 143	124 to 126	192 133 187	168 to 169	162 to 163

* The numbers here, and in the columns to the right, correspond to pages of the 1941 MIT report.

than many others. Load and time scales, though not shown on the oscillograms, can be taken from the tables of pages 176-181 of the report, and in this way a completely independent analysis of these records might be made by the reader.

The MIT authors carried out a reduction of the data in these records and the results are given in the tables of pages 182-192 of their report. The objectives were evaluation of yield point, maximum plastic load, and fracture load. Energy absorption was also found by determining an average load from the time record and multiplying by the elongation taken from the ruptured specimen after the test. These data are presented in the report without comment, and without explanation of the detailed methods used in their reduction.

1942 MIT REPORT

By the time the directive for the work of 1942 was written it was possible to be more explicit as to the purposes of the research. Of the four goals set, however, only the first was reached. It was stated in the contract as follows:

To determine the physical strength of medium steel at high rates of loading, with strain rates of 2000 inches per inch per second or more if possible.

The possibilities of obtaining high strain rates by applying moderate elongation rates to very short specimens were about exhausted in earlier work, and it became necessary to obtain higher elongation rates. Larger specimens were also desired, and the diameter was increased from the 0.20 inch previously used to 0.505 inch. Both tapered and notched specimens were used as before. In addition to load on time, elongation was also recorded, and by the elimination of time as a variable, a load elongation curve was obtained.

The plotting of curves from these data, however, raises some difficult questions. First, it is seen that since the strain rate increases throughout the process of elongation to rupture, the question of variation with strain rate can be considered only in connection with a specific value, such as strain rate at fracture. Then at high accelerations a correction is needed for the inertia of the parts intervening between the weigh bar and the section at which the stress is to be taken; see Figure 1 on page 5. This inertia plays a part in a phenomenon seen in all the records of both the 1941 and the 1942 reports, well shown in the sample record, Figure 7. It is an oscillation of high frequency and in many cases of even higher amplitude than in the sample record. What is seen is an oscillation of load, not of elongation. It was simply averaged out in the reduction of data in the 1941 report, but in 1942 this effect came in for consideration. The conclusion was that "the yielding of the test specimen sets up a train of elastic waves traveling longitudinally - regardless of how smoothly the elongation is applied."

Elastic waves superposed on a relatively uniform plastic flow pose a problem for further study. It is possible, however, that at the frequencies occurring, about 20,000 cycles per second, the limits of elastic action may be much higher than under actions involving lower time rates.

Figure 7 - Sample Oscillograph Record of Specimen 1N6 showing Load plotted on a basis of Time during Elongation

Experimental Details

The original intent in planning the 1942 program was to use a large 3-bar machine in which the hammer would be given a high velocity by a propellant explosive. Material for this use was assembled, but during the delays incident to completion of the task, a much more compact device for the same purpose was designed and built. This consisted of a cylindrical bomb of which the two halves were held together by the specimen. These halves enclosed a powder chamber with suitable provision for ignition; the resulting pressure forced them apart and broke the specimen. A sectional diagram of the device is given in Figure 8.

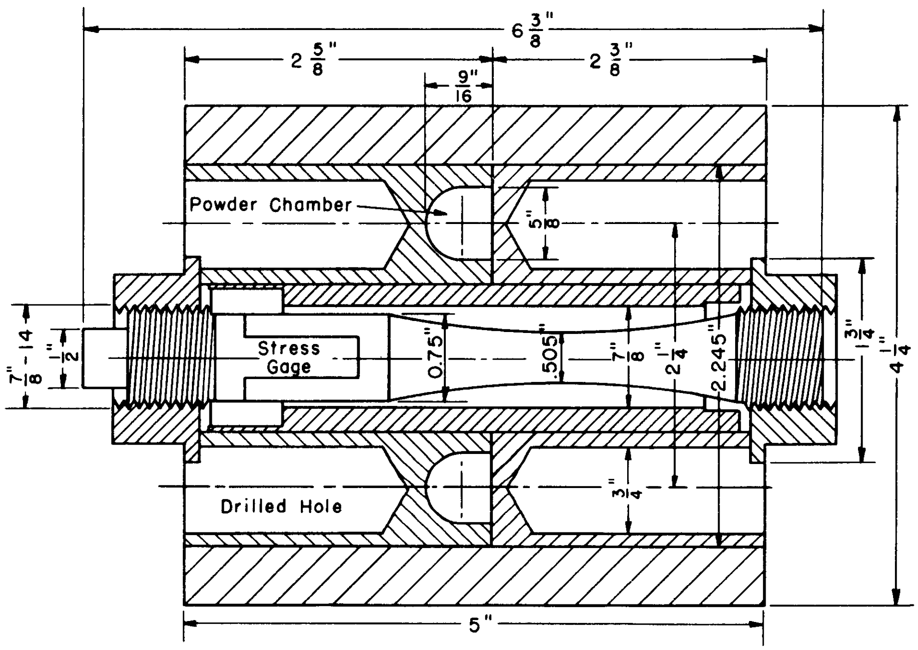

Figure 8. - Bomb-Type Impact Tester

The pressure of the powder was transmitted to the specimen through the massive heads forming the bomb. The elongation of the specimen therefore built up gradually, especially with low-order explosions. Detonating explosives were proposed, but not actually tried; it was supposed that in this way higher elongation rates could be obtained.

The forms of the specimens followed closely those shown in Figure 1, and detailed dimensions are given in Figures 18 and 19 of the 1942 report, where they are also summarized photographically in Figures 16 and 17. Details of the series are given in Table 3, page 18 of this report.

Original Records

The oscillograms obtained in 1942 were not as clear as those of 1941, presumably because of the higher writing speeds in the later work. Each of these oscillograms consisted of two synchronized records, one of overall elongation, and one of load from the weigh bar. The originals are not suitable for reproduction. The load-time record is similar to that seen in Figure 7, but the action of the bomb seems distinctly less smooth and regular than that of the lower speed tests of 1941. Some of the elongation records from Figure 23 of the 1942 report are reproduced herewith as Figure 9.

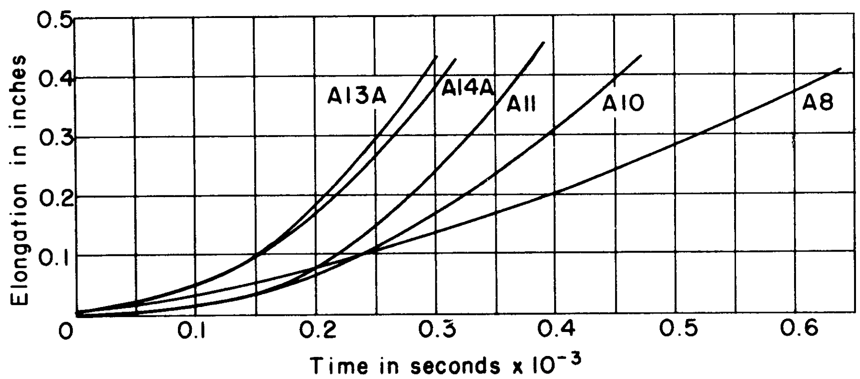

Figure 9 - Elongation-Time Records as Traced from Oscillograms

These are taken from Figure 23 of the 1942 report.

Figure 23 of the report also gives the results of differentiating the curves shown here in Figure 9. This was done partly to obtain accelerations for use in load corrections, though the manner in which this was done is not explained. The curve of velocity of elongation on time would be related to strain rate if the specimen were cylindrical and the strain uniform. In the tapered specimen, however, this is far from true; the strain rate at the fracture section must rise to a high but undetermined value. The curves of Figures 23 and 24 of the report, obtained by differentiation, are not reproduced here.

The data from the two records of load and of elongation are combined in load-elongation curves in Figure 32 of the 1942 report, reproduced here as Figure 10, and some numerical data from the same source are also included here.

The energy values in column 4 of Table 2, reduced to the same units used elsewhere in the present report, have been compared by the evaluation of an "Energy Ratio" which increases with the strain rate. The comparison is purely relative, however, as the circumstances of the test do not permit evaluation of actual strain rates, which vary from one section to another. At the fracture section the local value of strain rate may have risen to very high values, far above the averages quoted in Table 2.

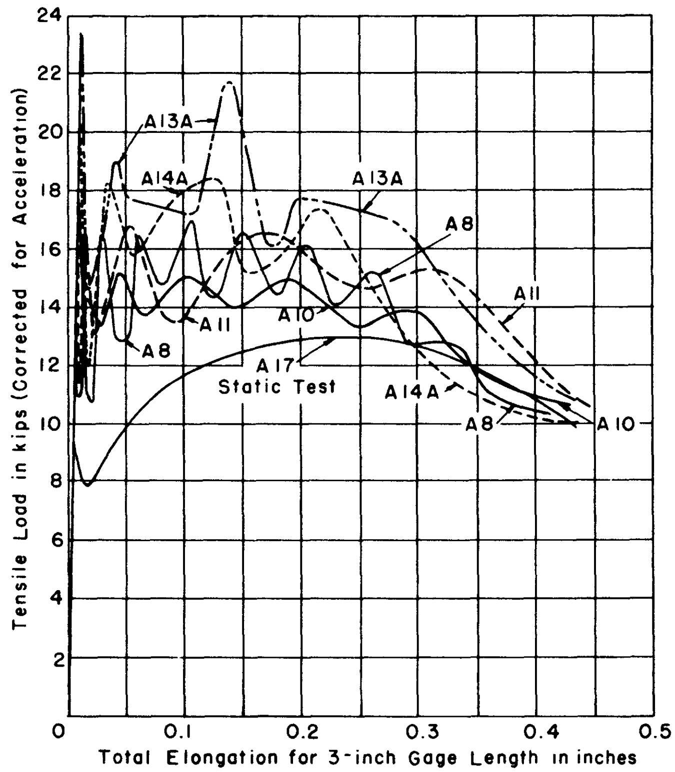

Figure 10 - Load-Elongation Curves plotted by Eliminating Time as a Variable in the Oscillograph Records of Load and Elongation on Time

This is Figure 32 of the 1942 report, which is also the source of the data in Table 2. Table 2 was part of this figure in the 1942 report. Strains, in inches per inch, may be obtained by dividing the elongation values by 3.

TABLE 2

Tabulated Data accompanying Figure 10

Specimen	Average Strain Rate* in/in/sec v_p	Speed of Loading* in/sec V_p	Energy** Absorbed in-kips/lb	Energy Ratio†	Fracture Load Ratio†
A8	1350	640	27	1.12	1.16
A10	1890	900	27	1.13	1.22
A11	2380	1150	30.5	1.28	1.30
A13A	3040	1430	33.3	1.40	1.24
A14A	2700	1340	29.4	1.23	1.20
A17	0	0	23.7	1.00	1.00

* From Table 1 of the report.

** Converted from foot-pound values.

† Based upon the results from the static test specimen A17.

A sample curve sheet, Figure 29 of the 1942 report, showing a comparison of the static and dynamic stress-strain curves from three tapered specimens, has been chosen for reproduction as Figure 11. One of the specimens, A2, was tested statically, and true stress and true strain as plotted were obtained as described in detail on pages 5 to 9 of this report.

The other two specimens, A10 and A11, were broken by impact. For each of these, two curves are drawn, corresponding to those shown in Figures 6 and 10. The value of maximum plastic load P_{max} was taken from the oscillograms, as indicated for Specimen A10 on page 68 of the MIT report. Combined with areas derived from measurements of diameter at various stations on the tapered specimen, it gives the data which are plotted as solid circles in Figure 11.

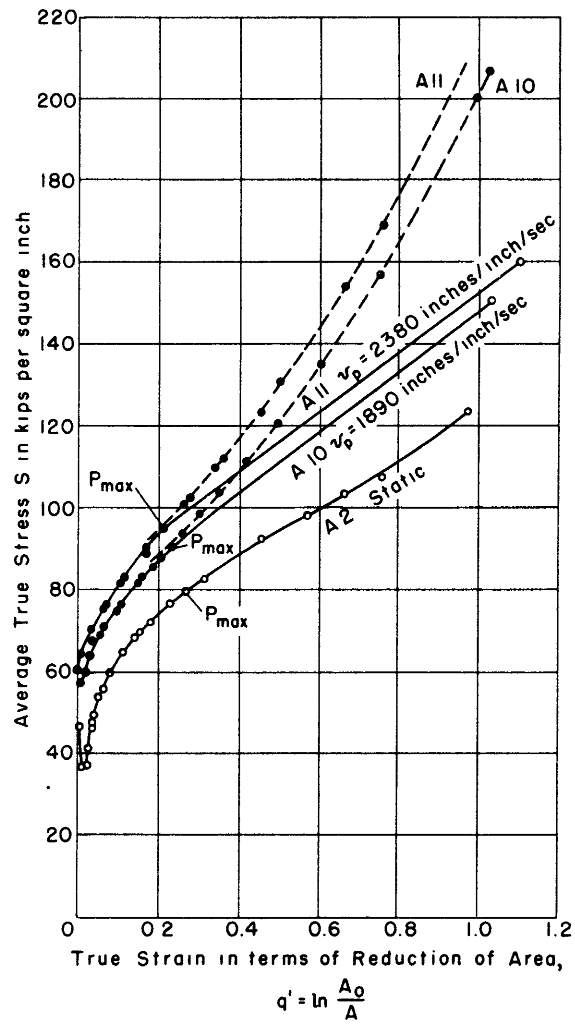

Figure 11 - Typical Stress-Strain Curves

These are taken from Figure 29 of the 1942 report. The open circles were plotted from data taken at the fracture section. v_p is the average strain rate from yield to fracture.

The stress *at the fracture section* after the load begins to diminish would be found by dividing this reduced load by the area at that section as both continue to diminish, if these quantities were known. The maximum true stress there is thus found by dividing the load at fracture by the area at fracture after the release of the load. In Specimen A10 the load, taken from the final line of the oscillograph data on page 68 of the 1942 report, is 10,600 pounds. The area, taken from the neck between Stations 18 and 19 as shown on page 82 is 0.0707 square inch. Since the initial area at the fracture section was 0.200 inch the true plastic strain was $\ln \frac{0.200}{0.0707} = 1.035$. The fracture stress, 150 kips per square inch, is then plotted in Figure 11 at a strain value of 1.035 inch per inch, taken from page 82 of the MIT report.

The stress-strain curve below the transition point is outlined by the solid circles. Above that point it is the straight line joining the transition point at maximum load with the fracture point. The taper in the necked section happened to be gradual enough to provide a number of spots above the transition point, which are plotted to show the approximate curve found by ignoring load reduction during necking. The error in comparison with the straight-line curve of true stress is clearly shown.

The question as to how much increase in strain rate caused the rise in the true stress-strain curve for specimens A10 and A11, shown in Figure 11, cannot be answered with certainty. The curves apply to the fracture section, though the data for low loads were taken from measurements at other sections (see MacGregor's hypothesis, page 22). The strain rate at the fracture section rises progressively during the test, but the peak value to which it rises may be many times the averages quoted in Table 2 of this report.

To facilitate reference to the original records, the specimens tested are listed in Table 3. Various data are summarized in Table 1 on page 29 of the 1942 MIT report.

TABLE 3

Index to Tensile Impact Data in the 1942 MIT Report

Designation	Number of Specimens	Static Specimens	Dynamic Specimens	Notch Length inch	Location of Photos* page	Location of Details page	Elongation-Time Curves page	Stress-Strain Curves page	Stress-Strain Tables page	Oscillograms page	Oscillogram Data page
A	14	9	5	Tapered	14	40	45	50-53	79-92	56-59	67-71
B	3	1	2	2	2	41			93	60	
C	2	1	1	1	2	41			94	60	
D	4	1	3	1/2	2	41	46		95	61-62	72
E	4	1	3	1/4	2	41	46		96	62-63	73-74
F	3	1	2	1/8 U**	2	41	46		97	64	75
G	4	1	3	1/8 V**	2	41	46		98	65-66	76-78

* The numbers here, and in the columns to the right, correspond to pages of the 1942 MIT report.

** U indicates a notch with rounded bottom, and V one with an angular bottom.

Data on variation of strength with strain rate are assembled in Figures 25 to 27, pages 47 to 49, of the 1942 report. Of these Figure 25 is chosen for reproduction here as Figure 12.

RESULTS OF THE MIT TESTS

For the original data in detail, reference must be made to the original reports, as indexed in Tables 1 and 2 on pages 12 and 16 of this report.

The best data on strength as affected by strain rate are summarized in Figures 10 and 12 herewith.

At the Taylor Model Basin the emphasis has been placed very largely on energy absorption, and both MIT reports have been thoroughly combed for such information. The points at which it was found in the 1941 report are indexed in Table 1. In the 1942 report the only energy data reported are those included in Table 2 on page 16.

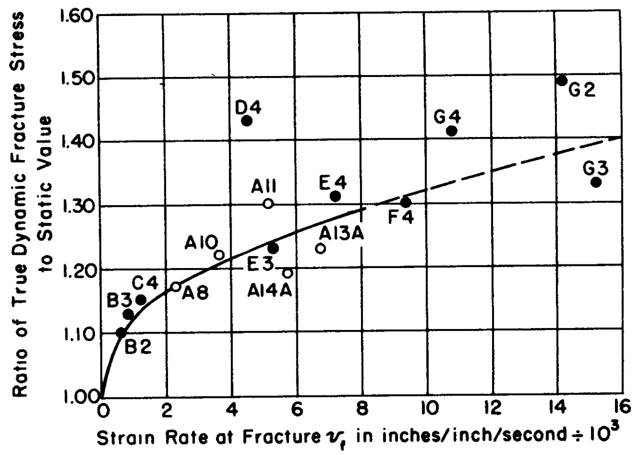

Figure 12 - Fracture Stress plotted on a basis of Strain Rate

This is Figure 25 of the 1942 MIT report.

For data on variation of energy absorption with strain rate, see Table 2 and Figure 13 of this report.

Although these data are plotted on strain rate, the high values are obtained only by the use of short notches. The variation of energy absorption explicitly with notch length is shown in Figures 14 and 15 following.

For other tests in which rate of loading and notch length are both varied, see Figures 15 and 16 following.

THE 1941 ENERGY DATA

These are of four kinds, taken up separately as follows.

Static Tests

Specimens 1 and 2 in each of the seven series of specimens were given a static load to failure, with measurements of minimum diameter in the neck at a series of measured loads. From these data true stress-strain data were plotted and energy values were found by integration. The value of the energy absorption Ω in inch-kips per pound of metal is thus evaluated for the most strained section, with the results given in Table 4.

TABLE 4

Energy Absorption under Static Load 1941 MIT Report

Ω, in inch-kips per pound of metal at section of greatest strain

Specimen	Ω	Specimen	Ω
1-A1	405	3-N2	408
1-A2	453	4-N1	459
1-N1	404	4-N2	436
1-N2	423	5-N1	464
2-N1	447	5-N2	450
2-N2	443	6-N1	446
3-N1	450	6-N2	460

Dynamic Tests on Notched Specimens

Energy values are quoted on pages 182 to 187 and again on pages 191 and 192 of the 1941 MIT report; corresponding values of strain rate are given on pages 171 to 181. Numerous errors and discrepancies were found, but by correction of some of the errors and choice of the values considered most likely to be correct, Table 5 has been made up.

TABLE 5

Energy Absorption Ω and Strain Rate $\dot{\epsilon}_0$ in Notched Specimens, 1941 Report

Ω in inch-kips per pound of metal
$\dot{\epsilon}_0$ in inches per inch per second

Specimen	Series											
	1N		2N		3N		4N		5N		6N	
	Notch Length											
	1/4 inch		3/8 inch		1/2 inch		3/4 inch		1 inch		1 1/2 inch	
	$\dot{\epsilon}_0$	Ω	$\dot{\epsilon}_0$	Ω	$\dot{\epsilon}_0$	Ω	$\dot{\epsilon}_0$	Ω	$\dot{\epsilon}_0$	Ω	$\dot{\epsilon}_0$	Ω
3					190	132	115	113.7			92	86.7
4	225	149	260	140.8	190	135.5	104	105.6	127	132	75	110.8
5	464	148.5	346	140.8	331	133.2	193	123.2	103	100.3	119	103.7
6	490	161	346	139	330	120.2	203	115			119	114.1
7	694	169.7	463	137.6	390	125.7	259	128.7	137	112.5	133	144.1
8			452	138.7	390	133.2	259	122.2	110	111.2	152	107.4
9	673	166.3	561	123.5	448	126.1	302	123.3	188	100.5	139	100.8
10	752	164.2	578	138	469	136.8	328	126.7	188	116.6	140	108.1
11	891	163.7	335	154.6	233	113.4	148	108.4	228	107.8	62	89.8
12	470	144.2	118	131.5	88	148.5	69	91	205	120.3		

Each of these values of energy per pound of metal is an average extended over the whole length of the specimen. The values were obtained by evaluating the average load by oscillograph and multiplying by the observed elongation. Strains also are averages for the whole length of the notch.

These data have been plotted in Figure 13, where some average values have been indicated by solid circles. These turn out somewhat differently, if averaged by strain rates, than if all the data from each series are grouped together. Both energy values and strain rates rise as the notch length diminishes, and if the data were precise enough to permit extrapolation to zero notch length, an average value comparable with those in Table 4 might be obtained.

In Figure 14 the averages of total energy absorption W for each notch length are plotted and the curve is extrapolated to zero notch length, where Ω is found by evaluation of the limiting values of the slope to have the value 253 inch-kips per pound of metal.

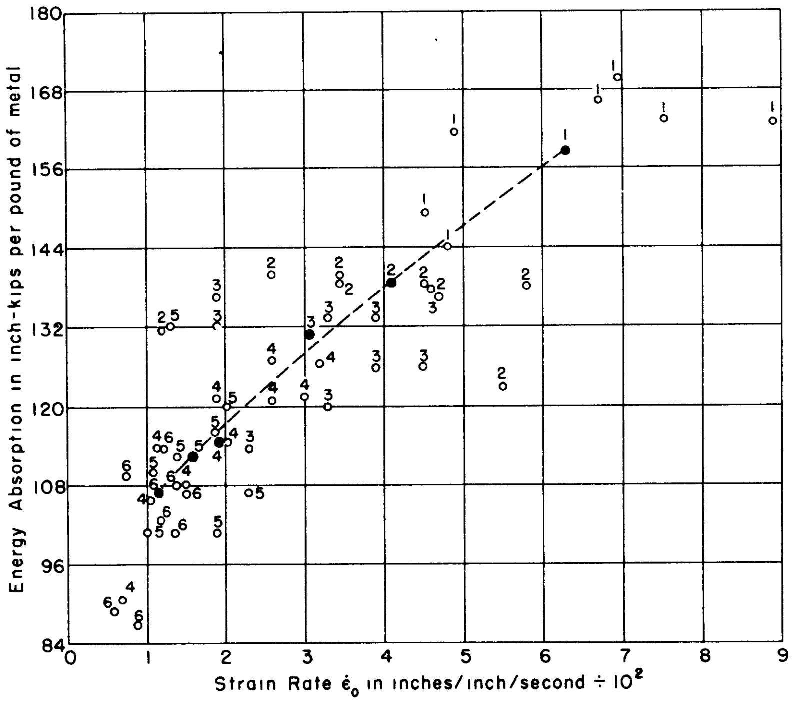

Figure 13 - Energy Absorption in Notched Specimens Plotted on Strain Rate

The number indicates the series number of the notched specimen. Each dot is the average for a series of the same notch length. The strain rate values used are those in Table 5 which is compiled from the tables of pages 176-181 of the 1941 report. These are obtained by dividing the duration into the ordinary ultimate strain, $\frac{L - L_0}{L_0}$. They thus represent an average, both as to elongation and time, for "below the peak" values occurring in the neck.

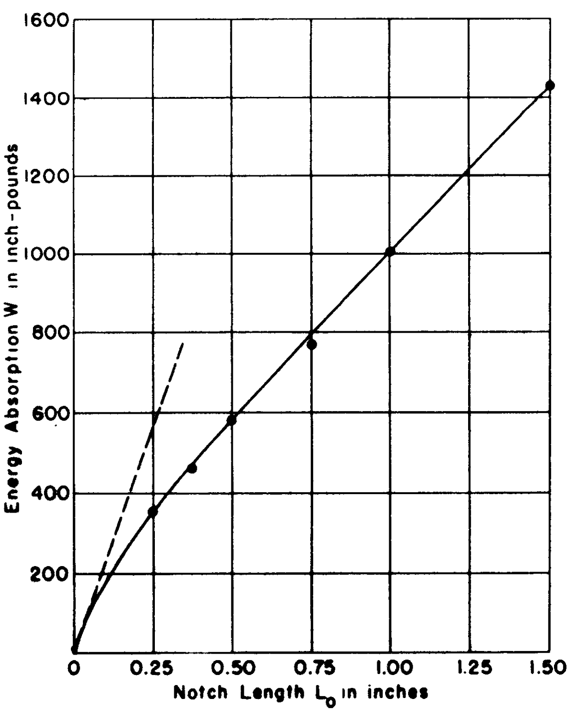

Figure 14 - Energy Absorption W in Notched Specimens, 1941 Data

The observed spots are averaged from the data on pages 191-192. The ordinate is total energy W; to obtain Ω it is necessary to divide by the weight of the metal in the notch. The limiting value of Ω is found from the slope of the curve at the origin.

The equation of the fitted curve is

$$W = 853 L_0 + 156 \left(1 - e^{-9L_0}\right),$$

where L_0 is expressed in inches.

The extrapolated value of Ω at a notch length of zero, as inferred from the limiting slope, is 253 inch-kips per pound.

Dynamic Tests on Tapered Specimens

By measurement after rupture of the residual reduction in area at a series of sections, following MacGregor's procedure, a stress-strain curve is obtained. Although each spot on this curve applies to a different section, the metal is presumably fairly homogeneous, and the curve is thus valid for the necked section at which the metal is the most severely worked. This presumption may be called MacGregor's hypothesis.*

The data from the tapered specimens were plotted and it was found not possible to strike in straight lines complying with MacGregor's condition of tangency at the point of inflection - the transition points of Figures 3 and 5 - and passing through the point of true stress at rupture. The lines were drawn to an estimated point of inflection without regard to tangency, and the resulting curve was integrated. The energy values so obtained are given in Table 6. They apply to the most strained section, where the strain rate also has a high value. The derived values of Ω afford some confirmation of the data in Table 4 on page 19.

TABLE 6

Energy Absorption Ω at Section of Greatest Strain in Tapered Specimens

1941 MIT Report

inch-kips per pound of metal

Specimen	Ω	Specimen	Ω
1-A3	539	1-A9	441
1-A4	618	1-A10	426
1-A6	684	1-A11	477
1-A7	494	1-A12	630
1-A8	430		

Izod Specimens

The curve of energy absorption on notch length, mentioned on page 11 in this report, when extrapolated to zero by the formula explained on page 25, leads to the value 183.5 inch-kips per pound.

THE 1942 ENERGY DATA

The 1942 values of plastic strain energy as given in the MIT report are given in Table 2, page 16, herewith for five tapered specimens under dynamic test. These values are low, ranging from 23.7 for static test to 33.3 inch-kips per pound at a strain rate of 3000 inches per inch per second. Energy values for notched specimens were not evaluated by the MIT authors.

OTHER COMPARABLE WORK

Additional sources of information on this subject are available in published form in References (9), (10), (12), (18), and (19).

---

* There is, however, no corresponding presumption as to strain rate, which will have widely different values at the different sections.

NADAI, CLARK

In these cases numerous tests on other metals were made, those on medium steel forming only a small part of the task. Load was applied mechanically through a retractable claw on a fast-moving flywheel. While Manjoine and Nadai (9) (10) report mainly ultimate stress and elongation at fracture, Clark (18) gives also yield point, energy absorption, and other data from the stress-strain curve.

By using in part unpublished data of the series of tests described in References (9) (10) a series of stress values for medium steel have been computed and are reproduced in the first three columns of Table 7.

TABLE 7

Energy Data of Manjoine and Nadai

The specimen length was 1 inch; its diameter was 0.200 inch.

Strain Rate	Yield Stress	Ultimate Stress	Estimated Average Stress	Per Cent Elongation	Energy
in/in/sec	kips/in²	kips/in²	kips/in²	in/in	in-kips/lb
10^{-6}	28	55.5	50	25.5	45*
10^{-5}	28.5	54	49	33	57
10^{-4}	30	53.5	49	38	66
10^{-3}	31	53.5	49	39.5	68.5
10^{-2}	33.5	54	50	39.5	70
10^{-1}	37	56	52	40	73.5
1	43	60	57	40	80.5
10	54.5	65.5	63	40	89
10^{2}	67	72.5	71	40	100
10^{3}	79	80.5	80	40	113

* This value is low due to aging in the mild steel. This test lasted 70 minutes, and the elongation was cut down to 25 per cent at this very low rate.

The range of these tests covers strain rates from $10^{-6} \frac{1}{\text{sec}}$ to $10^{3} \frac{1}{\text{sec}}$.

Manjoine made use of a graph, not yet published, in which yield stress, ultimate stress, ratio of yield stress to ultimate stress, and elongation, are plotted against strain rate. The per cent elongation of the whole specimen was multiplied by the average stress, which was estimated from the values of the yield stress and the ultimate stress. The energy as given in the last column is the product of average stress and elongation, divided by the density of steel, 0.283 pounds per cubic inch.

Comparing the energies from these tests by Nadai and Manjoine at

$$\dot{\epsilon} = 10^{-3} \frac{\text{in/in}}{\text{sec}} \qquad \text{Energy} = 68.50 \frac{\text{in-kips}}{\text{lb}}$$

$$\dot{\epsilon} = 10^{2} \frac{\text{in/in}}{\text{sec}} \qquad \text{Energy} = 100 \frac{\text{in-kips}}{\text{lb}}$$

An increase of 46 per cent in energy is obtained when the rate of strain is multiplied by 10^5.

The energy absorption in Clark's specimen, 0.2 inch diameter by 1 inch length, is about 80 inch-kips per pound of metal, as determined by load-elongation measurements. The highest speed of loading was 150 feet per second, corresponding in this specimen to 1800 inches per inch per second. At this speed the energy value rose to about 90 inch-kips per pound.

The complete load-elongation data are given for only three specimens. When these data are reduced to true stress and true strain, and a stress-strain curve is plotted, the limiting energy in inch-kips per pound of metal is 340 in the static test, but it rises to over 500 at 150 feet per second.

Higher speeds of loading thus lead to higher values of strength but only in moderation; on this and on the absence of sharply critical values like those reported by Mann, both observers agree.

DUWEZ

Although it does not fall strictly within the limits of the present summary, the more recent work at the California Institute of Technology should also be mentioned (12). This is at present writing the latest of a series of theoretical and experimental treatments of the subject of residual deflections in a linear specimen after its traversal by a plastic wave. It shows that in specimens of sufficient length the curve of strength on speed of hammer does show a maximum beyond which increased speed causes reduction of strength, and that in specimens of sufficient length this reversal is in a way strongly reminiscent of the discontinuity or "critical speed" reported by Mann.

As a summary of the present state of progress in this matter, the authors' abstract of Reference (12) is quoted in full herewith:

> "This report describes experiments made on an SAE 1020 cold-rolled steel for the purpose of studying (i) the influence of specimen length upon the application of the von Kármán theory (11); (ii) the influence of specimen length upon the total energy, total elongation and strain distribution for impact velocities between 0 and 200 feet per second; and (iii) the influence

of impact velocity on the tensile properties of this particular steel. The results of the work show (i) that the critical velocity observed experimentally agrees with the computed value; (ii) that the velocity at which the maximum is observed in curves of total energy versus impact velocity is independent of the gage length, and that the length of the specimen must be greater than 4 inches in order that a definite maximum may be observed in these curves; and (iii) that the total energy-absorbing capacity of SAE 1020 cold-rolled steel increases with increasing impact velocity until the critical velocity is reached."

Present interest is confined to phenomena below the critical velocity. However the rediscovery and theoretical explanation of the critical velocity mark a capital development in the knowledge of impact; this is being very actively pursued in further work at Pasadena.

Special attention was given by both Mann and Duwez to the energy absorption (12). Mann obtained values for medium steel in good agreement with Clark's - about 80 inch-kips per pound on a 1-inch specimen. Higher values for shorter notch lengths will be found in Reference (19).

Duwez separates energy into two parts, one associated with uniform elongation of the specimen, and the other with the necked region. The uniform energy, as the first item is called, has average values in static tests of 17.4 inch-kips per pound for Lot 1 and only 9 for Lot 2 of steel. The other item, the energy of necking, is stated only as a gross amount of energy; its reduction to terms of energy per pound of metal was not done by the authors, and seems not directly feasible. It can, however, be inferred by extrapolation from the curve of energy variation with notch length. As plotted by Duwez, this assumes a finite energy on zero notch length, which thus represents energy absorbed in connection with the concentrations in adjacent metal caused by the notch. As a purely empirical alternative it is proposed rather to omit the energy absorbed in the metal adjoining the ends of the specimen; at all notch lengths other than zero this omitted item is ignored, and at zero notch the energy absorbed in the notch is necessarily zero. Instead of Duwez' expression

$$W = AL_0\omega + C$$

the alternative

$$W = AL_0\omega + C\,(1 - e^{-nL_0})$$

is now proposed. In these expressions

- W is the total energy absorbed in the notch
- A is the area of the reduced section in the notch
- L_0 is the original length of the notch
- ω is energy per unit volume in a long specimen, in foot-pounds per cubic inch
- n, C, are empirical constants.

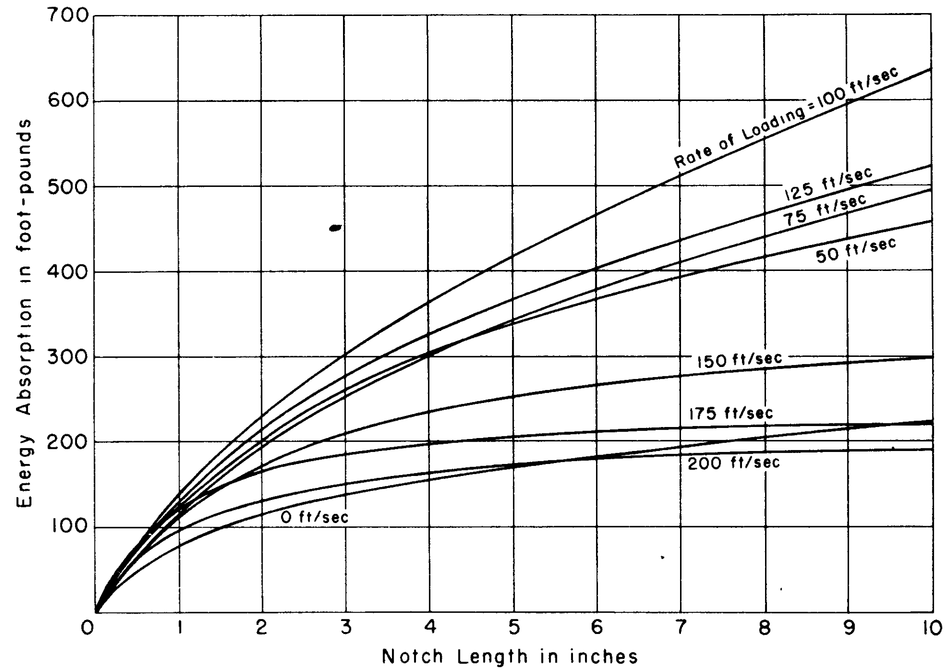

Figure 15 - Duwez' Data on Energy Absorption *W* Contours by Rate of Loading, plotted on Notch Length

In other analyses at the Taylor Model Basin, the symbol Ω is used to denote the energy per unit weight of metal in inch-kips per pound.

Ω is now observed to vary with L_o, approaching a constant value of the order of 10 inch-kips per pound as L_o increases. This constant depends on the material, having the value, as stated, of 17.4 in Duwez' Lot 1, and 9 in Lot 2.

TABLE 8

Energy Absorption at Various Rates of Loading, Duwez' Data

Rate of Loading feet per second	Ω inch-kips per pound
0	160.6
50	201.1
75	186.2
100	214.6
125	205.1
150	175.4
175	249.7
200	205.1

Special interest attaches to the value of Ω when $L_o = 0$; it is found from the expression

$$\left(\frac{W}{L_o}\right)_{L_o=0} = \left(\frac{dW}{dL_o}\right)_{L_o=0} = A\omega + nC$$

whence

$$\Omega = 42.4\left(\omega + \frac{nC}{A}\right)$$

Duwez' data are re-plotted in Figure 15. Extrapolation to zero notch length in each case leads to a series of values of Ω at different rates of loading as given in Table 8.

SUMMARY

CIT Data (18)

Values of load-elongation energy rise slightly, as the speeds of test increase, from about 80 at lower speeds to about 90 inch-kips per pound of metal at 150 feet per second. Local peak values rise to 340 inch-kips per pound, or even higher at higher speeds.

Watertown Data (3) (19)

Energy values, as obtained directly by the special method of observation used, are about 80 inch-kips per cubic inch of metal, on a 1-inch specimen.

Westinghouse Data (9) (10)

The data of Table 7 are shown in Figure 16.

Duwez' Data (12)

The data of Table 8 are shown in graphic form as Figure 17.

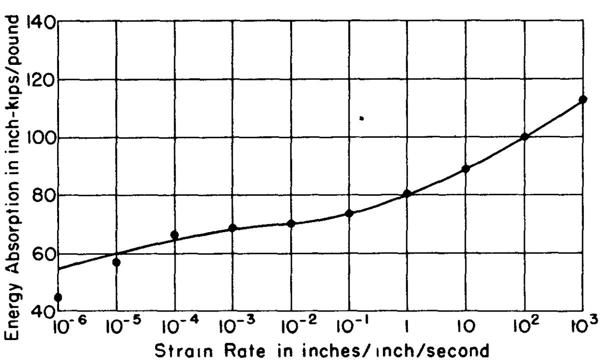

Figure 16 - Nadai's Data reduced to Terms of Energy Absorption

Table 7 shows details of calculation.

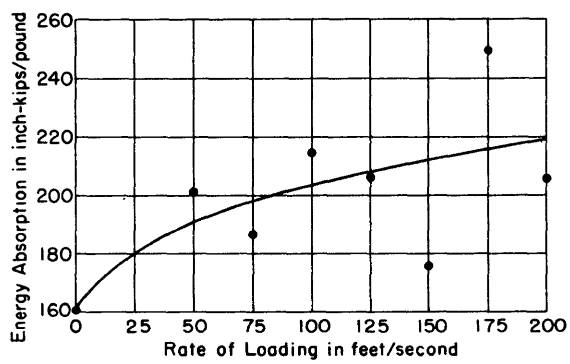

Figure 17 - Duwez' Energy Absorption at Zero Notch Length, Ω, Plotted on Rate of Loading

This curve differs from that of Figure 12 in that the ordinate is energy instead of stress and the abscissa is rate of loading, not strain rate.

COMMENT

EFFECT OF MODERATE TESTING SPEEDS

During the course of the MIT tests the opinion has gained ground that the effect of strain rate on the behavior of medium steel is quite moderate; in particular, at the strain rates involved in turrets and turret models, not over say 10^{-1} per second in the full scale and unity in the models,

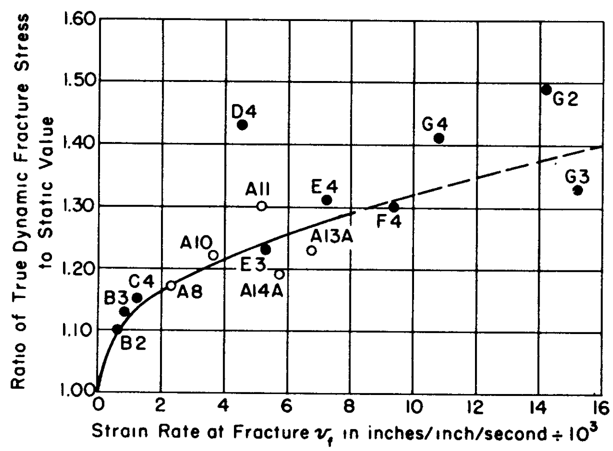

Figure 12 - Fracture Stress plotted on a basis of Strain Rate

This is Figure 25 of the 1942 MIT report.

the effect is negligible. Figure 12 confirms this opinion positively enough so that this question can be considered closed.

The data of Manjoine and Nadai, plotted in Figure 15, show positive indications of agreement with the foregoing MIT results.

The results obtained by Davis in Reference (20), are difficult to compare directly with the others because they were made under conditions of constant load rate rather than constant strain rate and because the center of interest lay in the yield point below which plastic flow is absent rather than the stress accompanying plastic flow. Rough values of slope of Davis' load-strain curves indicate that the overall strain rates did not exceed 10^{-1} per second, though local values may have been higher. The yield point was indicated to be of the order of 25 per cent higher at this strain rate than in static tests. This is difficult to reconcile with the other results, but in view of the circumstances it is considered not to invalidate the conclusion reached.

EFFECT OF HIGHER TESTING SPEEDS

The curve in Figure 12 is drawn with a slope diminishing upward on the supposition that the increase of plastic stress with strain rate falls off as the strain rate increases, so that the estimated increase over static stress is only 32 per cent at a strain rate of 10^4 per second.

Nadai, on the other hand, obtains a series of curves for medium steel at different temperatures, all of which show an upward turn at high strain rates. His curve for room temperature rises to values about 35 per cent above the static value at a strain rate of 10^3 per second, instead of about 10 per cent above as in the MIT results. At 10^4 per second (extrapolated) it is about 60 per cent above the static value instead of 32 per cent.

DEFINITION OF STRESS VALUE

The results mentioned in the foregoing are subject to the criticism that they are not wholly explicit as to the circumstances of stress determination. Nadai speaks of "ultimate stress" and deForest of "maximum stress" and of "dynamic fracture stress." It is apparent, however, that the true stress accompanying plastic flow continues to rise during the process of plastic elongation to rupture, whether or not there are definite yield points, upper or lower, either, both, or neither. The yield point, which plays so great a part in the action when confined to elastic limits, loses significance as plastic action increases. The steady rise of stress with strain in the plastic range is an effect of strain hardening, and for an evaluation of this neither the yield point nor any other single point on the plastic stress-strain curve is adequate. It is necessary, rather, to define the course of the stress-strain curve throughout the range extending from the limit of elastic action to the maximum load value. This is known as the "strain-hardening" range. The results of Nadai and those of deForest refer to its upper limit, the peak load point. The course of the curve beyond the strain-hardening range after necking begins is not yet defined, but an approximation is obtained by assuming linear variation of true stress with true strain, both for static and dynamic conditions of loading.

ENERGY ABSORPTION

Especial significance is to be attached to the integrated area of the true stress-strain curve, which equals the energy absorbed per unit volume of metal; when divided by the density, it equals the energy absorbed per unit weight of metal.

Take first the static data from the 1941 MIT report, relating to Specimens 1 and 2 of each of the seven series, for which stress-strain curves are available in Figures 156 to 169. The area under these curves varies little from a round value of 420 inch-kips per pound of metal. This is a peak value applying to the metal at the ruptured section, which received most drastic treatment. As soon as any metal outside the necked region is included in the average, the energy absorption per pound of metal is greatly reduced. Thus the values quoted on pages 191 and 192 for the dynamic tests of notched specimens are of the order of 150 inch-kips per pound of metal for the shortest notches, 1/4 inch. As longer specimens are considered, in which a large part of the metal is outside the necked region, the energy absorption drops below 100 inch-kips per pound.

Energy values are given in the 1942 MIT report only on page 54, as obtained from load-elongation curves of the tapered specimens. It is apparent that the metal is very incompletely worked, as the energy absorption taken over the whole specimen in the static case is only about 22 inch-kips per pound. From curves like that of Figure 6, however, a local value for the section at rupture may be found which confirms the similar values taken from the 1941 report, mentioned in the preceding paragraph.

The effect of increasing the rate of strain is to increase the energy absorption. Thus in Figure 11 the dynamic curve lies above the static curve throughout, so that the energy absorption is about 20 per cent higher than the static value in the case shown.

No account is taken here of the existence of a critical speed of loading above which energy absorption diminishes. Such an effect is of capital importance, and its details are being intensively studied at CIT. However no conclusions directly applicable to design of structures to resist dynamic load are as yet available.

Ostensibly, the data of pages 191 and 192 of the 1941 MIT report should also give quantitative information about the variation of energy absorption with the rate of strain, as given for the same tests on pages 176 to 181. A trend toward higher energy values at higher strain rates is soon apparent when the figures are reduced to energy per pound of metal, as in Figure 13 on page 21. Such a conclusion would be erroneous, however, since the high strain rates are there obtained only by use of short notches; when the notch length is increased not only is the strain rate reduced, but the part of the metal which does not share the most severe working effect is increased. These two effects are inseparable, and for this reason the use of short notches for obtaining high strain rates is not satisfactory.

The 1942 MIT series of tapered specimens is free from this objection, however, and the energy data of Table 2 on page 16 should be valid; the values range from 23.7 to 33.3 inch-kips per pound. These also show an increase of energy absorption with increasing strain rate; this is to be considered as the definitive result indicated by the MIT tests. As to the extent of this increase no very definite figures have been obtained, but the differences between static and high speed loading will hardly exceed 50 per cent.

OSCILLATIONS

An outstanding feature of all oscillograms of load on time is the cyclic nature of the record. The initial peak is followed by a large drop of load, in extreme cases as far as to half the peak value; this is followed by a damped oscillation about a quasi-stationary mean point. This phenomenon has been noted by all observers in the field. It was at first attributed to vibrations of elastic parts of the mechanical loading system, and was regarded as evidence of the complexity of the phenomena. This might, however, be disregarded if a mean line were passed through the cyclic record; a similar technique has been applied in the analysis of the behavior of elastic diaphragms used with success for measuring transient pressures which set the diaphragm itself in vibration.

Meanwhile it was thought possible that the initial load surge might be reduced by the use of a propellant powder for loading.

However, the oscillations still appeared in the 1942 MIT data taken with the bomb. DeForest concluded that "the irregular contour of the dynamic stress-strain curves is caused not by the conditions of loading but by the initial longitudinal impulse set up by the sudden drop in load at the lower yield point. In other words, the yielding of the test specimen sets up a train of elastic waves traveling longitudinally of the test specimen regardless of how smoothly the elongation is applied."

This conclusion, however, does not eliminate the possibility of overshoot in load, caused by its abrupt application. As the speed of loading becomes higher, this overshoot will naturally become greater; it may be mainly this phenomenon which is reported as an increased yield point at increased rates of loading.

CLOSING COMMENT

The 1941 MIT oscillograms, a sample of which was shown in Figure 7 on page 11, consistently show initial maxima higher than the subsequent "ultimate load" value. This initial maximum is tabulated as "yield point" and the subsequent lower maximum as "maximum load" in the tables of pages 191 and 192.

This appears to be anomalous and it raises a question as to what might be expected if a specimen were loaded to a value intermediate between the yield point and the subsequent lower maximum value. Presumably plastic flow would not begin if the yield point were not attained, and since, as seen in Figure 10, page 16, the stress may rise to high values without reaching the upper yield point, quick release may permit the application of loads far above the "ultimate strength" without causing any plastic flow at all.

This anomaly can hardly be explained away, as has been done in some cases, by attributing it to "instrumental vibrations" and by assuming that the mean line through the cyclic record represents the true variation of load with time.

The 1942 MIT data in Figure 10, page 16, present the basis for such general conclusion as is possible about the effect of fast loading; they show that fast loading increases the initial maximum very greatly, but that the load-elongation curves for all rates of loading, including the static case, converge at about the same value of fracture load.

Thought at the Taylor Model Basin follows a somewhat different line, in placing emphasis, for structures subject to high-order transient load, not on load-bearing capacity but on energy-absorbing capacity. The limiting values of energy which can be absorbed locally may be as much as 500 inch-kips per pound of metal in medium steel. Averages taken over a whole specimen may be of the order of one-fiftieth as much, and in an extended assembled structure the averages may be expected to fall still lower.

From this point of view there is thus almost limitless room for an improvement in efficiency of such structures as torpedo protection systems. In a similar way the margin between actual and possible efficiencies of the steam engine was at one time so great that improvement has been limited only by the ingenuity needed to obtain it. Underwater protective systems, if improved by a fraction of the benefit now obtained by use of high steam pressures, will give a defensive superiority of proportionate military value. If a modification of metallurgical or structural practice could increase the energy absorbing capacity of a ship's side by 1/20 of the figure attained in the neck of a tensile specimen, the result would be a revolution in sea warfare.

REFERENCES

(1) Robert M. Vose in Marks' Handbook, Fourth Edition, page 424.

(2) 1922 Symposium on Impact Testing, Proceedings of the American Society for Testing Materials, vol. 22, 1922, pages 5 to 150, with bibliography.

(3) "High-Velocity Tension-Impact Tests," by H.C. Mann, Proceedings of the American Society for Testing Materials, vol. 36, II, 1936, pages 85 to 109.

(4) 1938 Symposium on Impact Testing, Proceedings of the American Society for Testing Materials, vol. 38, II, 1938, pages 1 to 177, including an article by Clark and Dätwyler, pages 98 to 111.

(5) "Some Complexities of Impact Strength," by A.V. deForest, American Institute of Mining and Metallurgical Engineers, Technical Publication, 1941, pages 1 to 17.

(6) "Festigkeitsprüfung bei Schlagartiger Beanspruchung" (Strength Testing under Impact Loading), by R. Mailänder, in Handbuch der Werkstoffprüfung, edited by E. Siebel, vol. 2, 1939, pages 129 to 165.

(7) "Concerning the Effect of Notches and Laws of Similitude in Material Testing," by A. Nadai and C.W. MacGregor, Proceedings of the American Society for Testing Materials, vol. 34, II, 1934, pages 216 to 228.

(8) "Prüfmaschinen und Einrichtungen für Stoszartige Beanspruchung" (Testing Machines and Arrangements for Impact Loading), by E. Lehr, Handbuch der Werkstoffprüfung, Siebel, vol. 1, 1940, pages 155 to 195.

(9) "High Speed Tension Tests at Elevated Temperatures," Part I, by M. Manjoine and A. Nadai, Proceedings of the American Society for Testing Materials, vol. 40, II, 1940, pages 822 to 839, with discussion by Lessels. As a matter of historical interest, Dr. Nadai calls special attention to some early investigations in this field, to which specific reference is made in this article. Names and dates are as follows: Ludwik (1909), Cassebaum (1911), R. Plank (1912), Koerber and Storp (1925), E. Meyer (1927), Siebel and Pomp (1928), Deutler (1932), Brinkmann (1933), Honegger (1935).

(10) Continuation of Reference (7), Parts II and III, Journal of Applied Mechanics, vol. 8, 1941, pages 77 to 91. See also discussion in vol. 9, 1942, pages 45 to 47.

(11) "Propagation of Plastic Waves," by Th. von Kármán, H.F. Bohnenblust, and D.H. Hyers, National Defense Research Committee, A-103. Contains further references to the work of G.I. Taylor, M.P. White, and L. Griffis.

(12) "Influence of Specimen Length on Strain Propagation in Tension," by Duwez, Wood, and Clark, National Defense Research Committee, A-105.

(13) "Model Investigation of Armored Structures," by Lt. R.D. Conrad, Construction and Repair Bulletin 13-A, 1940.

(14) "Report on Impact Research," by A.V. deForest, A.R. Anderson, and R. Fanning, May 1941. Only three copies of this report were furnished under the contract. One of these is filed at the Bureau of Ships; two are retained at the Taylor Model Basin.

(15) "Impact Research on Medium Steel," by A.V. deForest, C.W. MacGregor, and P.R. Shepler, September 1942. Nine copies, distributed as follows: 1 to Coordinator of Research and Development, Navy Department; 4 to Bureau of Ships; 3 retained at Taylor Model Basin; 1 furnished by author direct to National Defense Research Committee NS-109.

(16) "Electronic Methods of Observation at the David W. Taylor Model Basin, Part 1 - Dynamic Actions in Hull Structure," CONFIDENTIAL TMB Report R-45, October 1941.

(17) "A Two-Load Method of Determining the Average True Stress-Strain Curve in Tension," by C.W. MacGregor, Journal of Applied Mechanics, vol. 6, 1939, pages 156 to 158.

(18) "Influence of Impact Velocity on Tensile Characteristics of some Aircraft Metals and Alloys," by Donald S. Clark, National Advisory Committee for Aeronautics, Technical Note 868, October 1942.

(19) "Application of Tension Impact Tests," by G.F. Jenks, Transactions of the American Society of Mechanical Engineers, vol. 59, 1937, IS, pages 313 to 318.

(20) "The Effect of the Speed of Stretching and the Rate of Loading on the Yielding of Mild Steel," by E.A. Davis, Journal of Applied Mechanics, vol. 5, 1938, page 137.

(21) Symposium on the Tension Test. Proceedings of the American Society for Testing Materials, 1940, pages 501 to 642, including article by C.W. MacGregor, pages 508 to 534. MacGregor's article has an extensive bibliography.

(22) "Das Verhalten des Querkontraktionskoeffizienten des Eisens bis zu sehr groszen Dehnungen" (The Behavior of the Coefficient of Transverse Contraction of Iron up to Very Large Elongations), by R. Plank, Zeitschrift des Vereines deutscher Ingenieure, vol. 55, September 2, 1911, pages 1479 to 1483, and "Betrachtungen über Dynamische Zugbeanspruchung" (Observations on Dynamic Tensile Loading), by R. Plank, Zeitschrift des Vereines deutscher Ingenieure, vol. 56, January 6, 1912, pages 17 to 24.

APPENDIX

FORMULAS FOR TRUE PLASTIC STRAIN*

Consider a typical section of a test specimen in the *plastic* range, as shown in the accompanying sketch.

Here

A is the area,
A_o is the original area,
L is the length,
L_o is the original length,
ϵ is the strain, and
q' is the reduction in area.

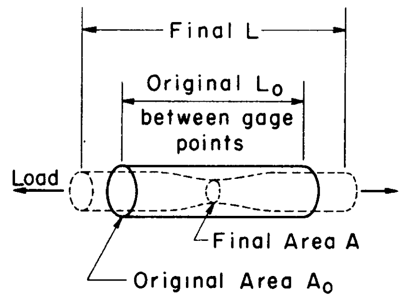

Following the orthodox procedure,

$\epsilon_o = \frac{L - L_o}{L_o} = q_1$, may be set down to represent the "ordinary" elongation, and

$\epsilon_1 = \frac{A_o - A}{A_o} = q_o$, the "ordinary" reduction of area.

Assuming that the volume of an element in the test section remains constant, or $A_oL_o = AL$, then $\frac{L - L_o}{L_o} = \frac{A_o - A}{A}$, and $\frac{A_o - A}{A_o} = \frac{L - L_o}{L}$.

So long as strains are small all these expressions are equivalent, but a third formula, also equivalent to the others when strain is small, is found useful. It is

$$\epsilon = \ln\frac{L}{L_o} = \ln\frac{A_o}{A} = q'$$

ϵ is called the true strain and q' the true reduction of area because in this case the change in length or area is referred neither to the initial nor the final value, but to the average of these two values. Thus, with good approximation,

$$\ln x = \frac{x - 1}{\frac{1}{2}(x + 1)} \quad \text{(See Peirce's Integral No. 767)}$$

so that if $x = \frac{A_o}{A}$

$$\ln\frac{A_o}{A} = \frac{A_o - A}{\frac{1}{2}(A_o + A)} = \frac{\text{actual reduction of area at fracture}}{\text{average area from start to fracture}}$$

and similarly if $x = \frac{L}{L_o}$.

---

* See Reference (21). The symbols used here are MacGregor's.

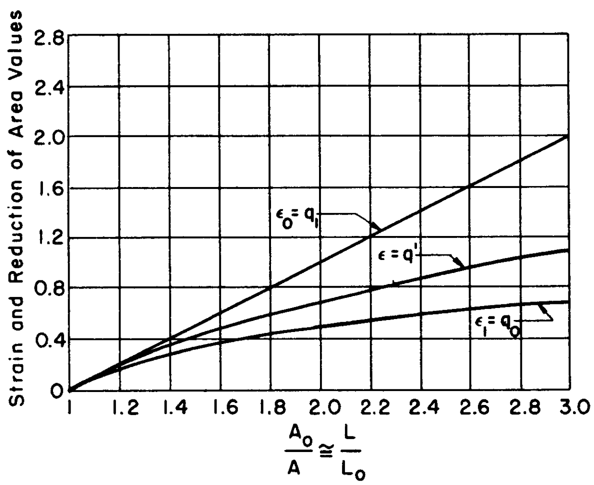

Figure 18 - Comparison of Strain and Reduction of Area Values for Various Amounts of Deformation

The logarithmic definition of strain ϵ thus has the merit of agreeing with the ordinary or conventional definitions $\epsilon_0 = \frac{\Delta L}{L_0}$ when the strain is infinitesimal, and at the same time of providing a true or natural value when the strain is finite by referring elongation to an average length rather than the initial or original value of L in case of ϵ_0 or to the value L attained after elongation is complete in case of ϵ_1. A similar statement may be made with respect to $q_0 = \frac{\Delta A}{A_0}$. The relations between these quantities are shown graphically in Figure 18.

The following relationship between ϵ, ϵ_0, and ϵ_1 may be obtained:

$$\epsilon = \ln (1 + \epsilon_0) = - \ln (1 - \epsilon_1)$$

Further, if

$$\epsilon_u = q_u' \text{ (at \underline{u}ltimate* load)} = \ln \frac{A_0}{A_u}$$

and

$$\epsilon_b = q_b' \text{ (at \underline{b}reaking point)} = \ln \frac{A_0}{A_b}$$

then defining

$$\epsilon_n = q_n' = \ln \frac{A_u}{A_b}$$

it will be found that

$$\epsilon_n = \epsilon_b - \epsilon_u$$

The plastic strains as thus defined are seen to be fully and directly additive.

---

* Maximum.